Electronic Supplementary Material

Efficient conversion of lignin to alkylphenols over highly stable inverse spinel $MnFe_2O_4$ catalysts

Yi Qi, Xuezhi Zeng, Lingyingzi Xiong, Xuliang Lin (✉), Bowen Liu, Yanlin Qin (✉)

Guangdong Provincial Key Laboratory of Plant Resources Biorefinery, School of Chemical Engineering and Light Industry, Guangdong University of Technology, Guangzhou 510006, China

E-mails: xllin@gdut.edu.cn (Lin X); ylqin@gdut.edu.cn (Qin Y)

Supporting Figures

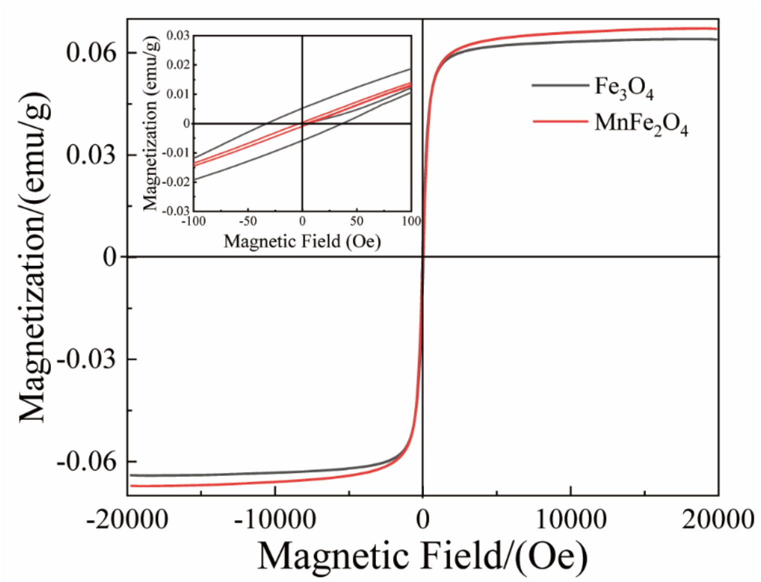

Fig. S1. M–H loops of the Fe_3O_4 and $MnFe_2O_4$ sheet. Inset shows the M–H loops at the low magnetic field (top left).

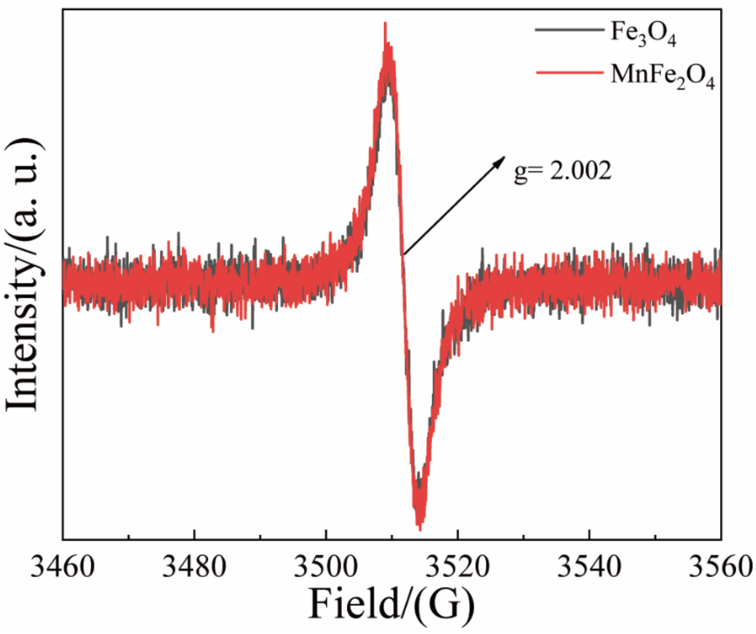

Fig. S2. EPR patterns of Fe_3O_4 and $MnFe_2O_4$.

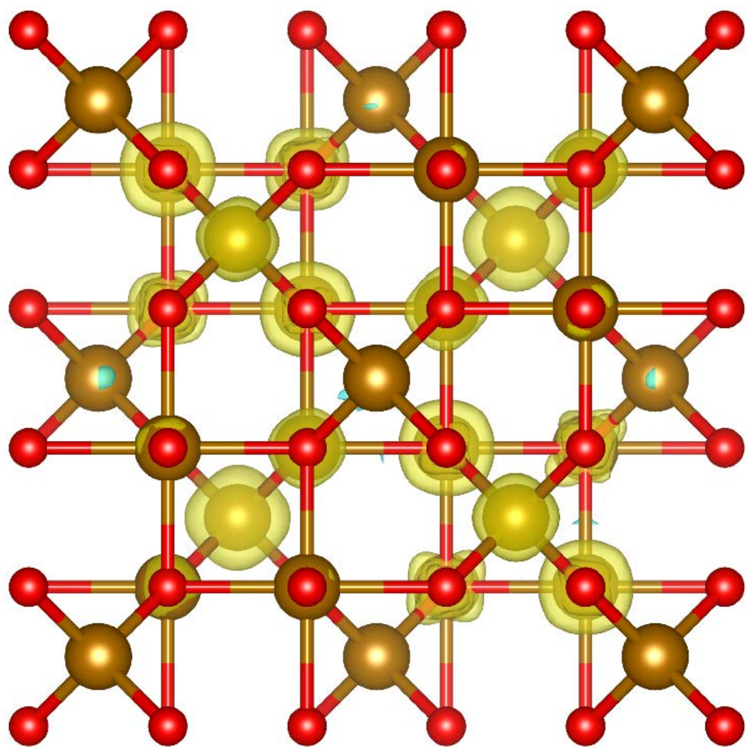

Fig. S3. Difference in charge density of Fe_3O_4 from DFT calculations, Fe atoms and O atoms are represented by golden and red balls, respectively.

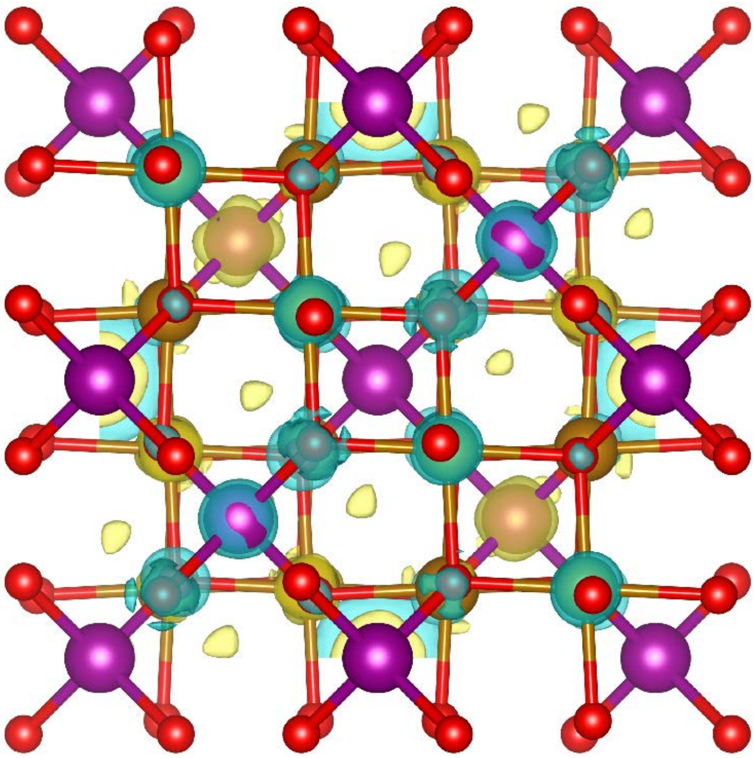

Fig. S4. Difference in charge density of $MnFe_2O_4$ from DFT calculations, Mn atoms, Fe atoms and O atoms are represented by purple, golden yellow and red balls, respectively.

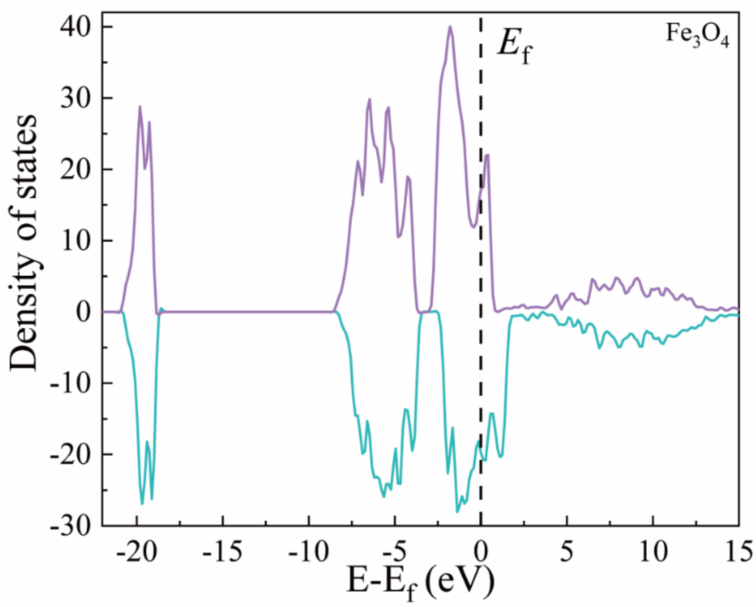

Fig. S5. Total density of states diagram for Fe_3O_4.

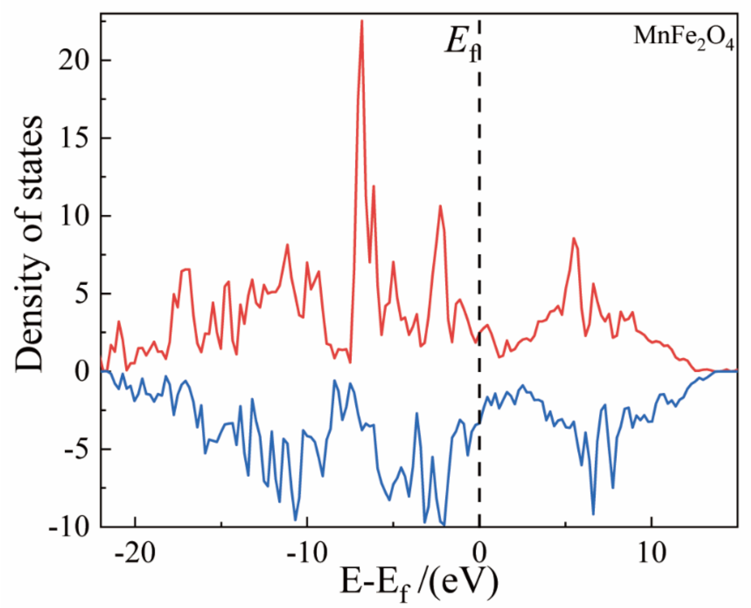

Fig. S6. Total density of states diagram for $MnFe_2O_4$.

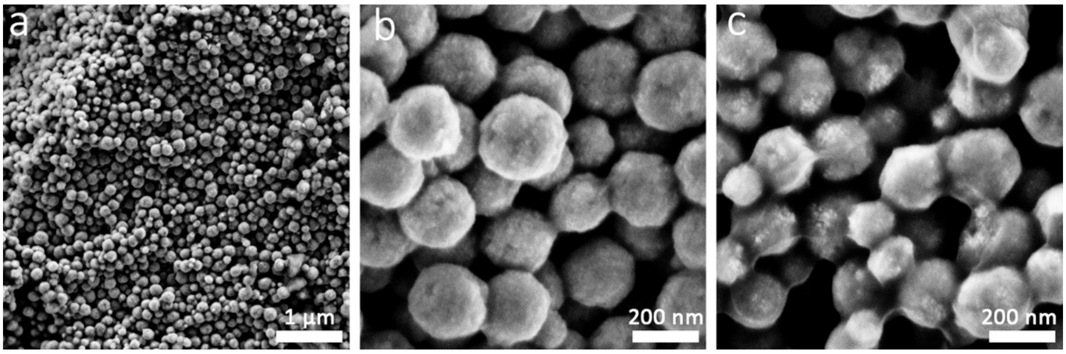

Fig. S7. SEM of $MnFe_2O_4$ after cyclic catalysis of lignin.

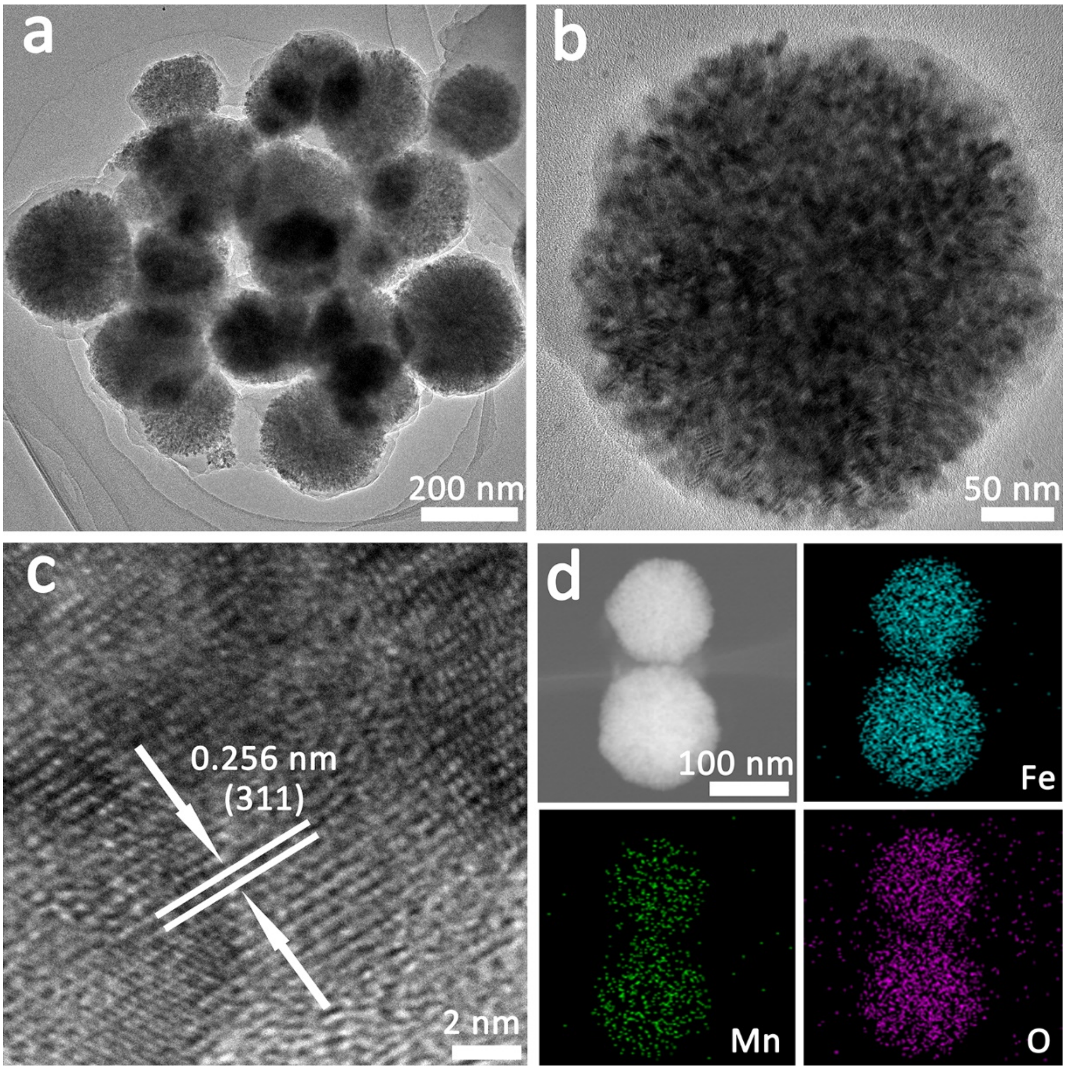

Fig. S8. $MnFe_2O_4$ after lignin cycle catalysis, (a, b) TEM images at different magnifications, (c) HRTEM images, (d) HAADF-STEM images and corresponding elemental mapping maps of Mn, Fe and O.

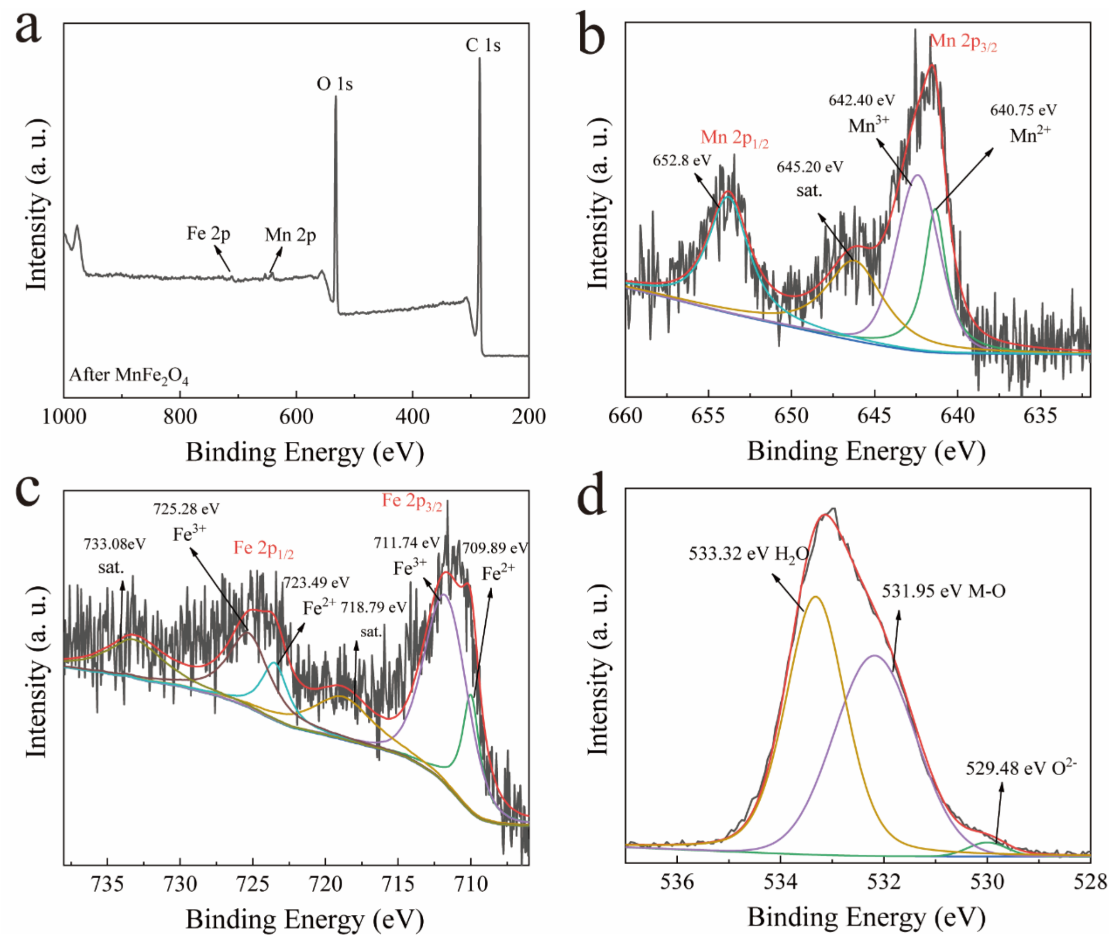

Fig. S9. $MnFe_2O_4$ after lignin cycle catalysis, (a) Full range XPS spectra (b) high-resolution Mn 2p spectra, (c) high-resolution Fe 2p spectra , (d) high-resolution O 1s spectra.

Table S1. Comparison of catalytic depolymerization of technical lignin.

Lignin	**Catalyst**	**Solvent**	**Response conditions**	**Conversion and Selectivity**	**Ref.**
Alkali lignin	$MnFe_2O_4$	Isopropanol	250 °C, 4h, 2 Mpa H_2	Conversions 94 w% , Alkyl phenol selection 90 w%	This work
Kraft lignin	H-$NiFe_2O_4$	Methanol and 1, 4-dioxane	320 °C, 24h, 2 Mpa H_2	Conversion 90 wt%, Selectivity 70 wt%	[S1]
Birch lignin	Pt/$NiAl_2O_4$	Water	280 °C,20 h, 2 Mpa N_2	25.2 wt%, 17.3 wt % yield of 4-alkylphenols	[S2]
Corncob lignin	$ZnMoO_4$/MCM-41	Methanol	220 °C, 4 h 30 Mpa	15 to 37.8 wt% phenolic monomers	[S3]
Enzymatic hydrolysis lignin	NiMo/γ-Al_2O_3	Cyclohexane	320 °C, 7.5 h, 3 Mpa H_2	cycloalkane yield of 104.4 mg/g, 44.4 wt% selectivity	[S4]
Sugarcane bagasse lignin	Fe-Pd/HZSM-5	Ethanol and water (1:1)	320 °C, 1 h, 1 Mpa H_2	Conversion 98.17%, Aromatic monomer selectivity 27.92%	[S5]

Raw lignin	Ni-Fe-Mo_2C/AC	H_2O and methanol	260 °C, 4 h, 3 Mpa H_2	yields of liquefaction (89.56%) and phenolic monomers (35.53%)	[S6]
Alkali lignin	Cu-Mg-Al mixed oxides	Ethanol	340 °C, 4 h, 1 Mpa N_2	yielded 36 wt % monomers	[S7]
Alkaline lignin	In situ-converted hierarchical analcime	H_2O	300 °C, 4 h	Conversion 92.5%, Yield Bio-oil 63.02%, Total phenol Yield 95.61%。	[S8]
Lignin	Pd-Zn/C	Methanol	225 °C, 12 h, 3.5 Mpa H_2	4-propyl-2,6-dimethoxyphenol formation at 71%	[S9]
Kraft lignin	MoO_3	1, 4-dioxane, isopropanol and methanol	280 °C, 6 h, 1 Mpa N_2	87 wt% yield of petroleum ether soluble products	[S10]
Enzymatic hydrolysis lignin (0.5 g)	Ni-Ru/Al_2O_3 (0.125 g)	Isopropanol	220 °C, 4 h, 1 Mpa N_2	Total SP yield of 58.1%	[S11]

References

[S1] D. Xiaomeng, L. Wenzhi, Z. Chaofeng, J. Xiao, Catalytic waste Kraft lignin hydrodeoxygenation to liquid fuels over a hollow Ni-Fe catalyst, Applied Catalysis B: Environmental, 287 (2021) 119975.

[S2] L. Li, L. Dong, D. Li, Y. Guo, X. Liu, Y. Wang, Hydrogen-Free Production of 4-Alkylphenols from Lignin via Self-Reforming-Driven Depolymerization and Hydrogenolysis, ACS Catalysis, 10 (2020) 15197-15206.

[S3] S. Wang, W. Gao, H. Li, L.P. Xiao, R.C. Sun, G. Song, Selective Fragmentation of Biorefinery Corncob Lignin into p-Hydroxycinnamic Esters with a Supported Zinc Molybdate Catalyst, ChemSusChem, 11 (2018) 2114-2123.

[S4] Q. Liu, Y. Bai, H. Chen, M. Chen, Y. Sang, K. Wu, Z. Ma, Y. Ma, Y. Li, Catalytic conversion of enzymatic hydrolysis lignin into cycloalkanes over a gamma-alumina supported nickel molybdenum alloy catalyst, Bioresour Technol, 323 (2021) 124634.

[S5] Z. Zeng, J. Xie, Y. Guo, R. Rao, B. Chen, L. Cheng, Y. Xie, X. Ouyang, Hydrogenolysis of lignin to produce aromatic monomers over Fe Pd bimetallic catalyst supported on HZSM-5, Fuel Processing Technology, 213 (2021) 106713.

[S6] B. Yan, X. Lin, Z. Chen, Q. Cai, S. Zhang, Selective production of phenolic monomers via high efficient lignin depolymerization with a carbon based nickel-iron-molybdenum carbide catalyst under mild conditions, Bioresour Technol, 321 (2021) 124503.

[S7] X. Huang, C. Atay, T.I. Korányi, M.D. Boot, E.J.M. Hensen, Role of Cu–Mg–Al Mixed Oxide Catalysts in Lignin Depolymerization in Supercritical Ethanol, ACS Catalysis, 5 (2015) 7359-7370.

[S8] J. Zhang, Y. Ge, Z. Li, Synchronous catalytic depolymerization of alkaline lignin to monophenols with in situ-converted hierarchical zeolite for bio-polyurethane production, International Journal of Biological Macromolecules, 215 (2022) 477-488.

[S9] B. Liu, M. Sanchez, J. Truong, P.C. Ford, M.M. Abu-Omar, Catalytic conversion of high S-lignin to a sustainable tri-epoxide polymer precursor, Green Chemistry, 24 (2022) 4958-4968.

[S10] B. Tang, W. Li, X. Zhang, B. Zhang, H. Zhang, C. Li, Depolymerization of Kraft lignin to liquid fuels with MoS_2 derived oxygen-vacancy-enriched MoO_3 in a hydrogen-donor solvent system, Fuel, 324 (2022) 124674.
[S11] H.-T. Wang, Z.-K. Li, H.-L. Yan, Z.-P. Lei, J.-C. Yan, S.-B. Ren, Z.-C. Wang, S.-G. Kang, H.-F. Shui, Catalytic hydrogenolysis of lignin and model compounds over highly dispersed Ni-Ru/Al_2O_3 without additional H_2, Fuel, 326 (2022) 125027.